AFRL-OSR-VA-TR-2014-0184

Colloidal Metamaterials at Optical Frequencies

Jennifer Dionne
LELAND STANFORD JUNIOR UNIV CA

07/18/2014
Final Report

Air Force Research Laboratory
AF Office Of Scientific Research (AFOSR)/ RTD
Arlington, Virginia 22203
Air Force Materiel Command

REPORT DOCUMENTATION PAGE

Form Approved
OMB No. 0704-0188

1. REPORT DATE *(DD-MM-YYYY)*	**2. REPORT TYPE**	**3. DATES COVERED** *(From - To)*
08-07-2014	Final	31-03-2011 - 31-03-2014

4. TITLE AND SUBTITLE

Colloidal Metamaterials at Optical Frequencies

5a. CONTRACT NUMBER

5b. GRANT NUMBER
FA9550-11-1-0024

5c. PROGRAM ELEMENT NUMBER
61102F

6. AUTHOR(S)

Jennifer A. Dionne

5d. PROJECT NUMBER

5e. TASK NUMBER

5f. WORK UNIT NUMBER

7. PERFORMING ORGANIZATION NAME(S) AND ADDRESS(ES)

Stanford University
340 Panama Street
Stanford, CA 94305-4100

8. PERFORMING ORGANIZATION REPORT NUMBER

9. SPONSORING / MONITORING AGENCY NAME(S) AND ADDRESS(ES)

Air Force Office of Scientific Research
875 N. Randolph Street
Suite 325, Room 3112
Arlington, VA 22203-1768

10. SPONSOR/MONITOR'S ACRONYM(S)

AFOSR

11. SPONSOR/MONITOR'S REPORT NUMBER(S)

12. DISTRIBUTION / AVAILABILITY STATEMENT

Distribution A

13. SUPPLEMENTARY NOTES

N/A

14. ABSTRACT

To date, almost all reported metamaterials have been fabricated with top- down nanofabrication techniques, which are severely limited in scale and throughput, are inherently limited to planar geometries, and are inherently solid-state materials. Our team has combined theoretical and experimental methods to produce a colloidally-synthesized metamaterial fluid, or "metafluid" exhibiting strong electric and magnetic resonances at visible frequencies. Our metafluid combines the advantages of solution-based processing with facile integration into conventional optical components. Protein-antibody interactions are used to direct the solution-phase self-assembly of discrete metamolecules comprised of silver nanoparticles tightly packed around a single dielectric core. The electric and magnetic response of individual metamolecules and the bulk metamaterial solution are directly probed with optical scattering and spectroscopy. Effective medium calculations indicate that the bulk metamaterial exhibits a negative effective permeability and a negative refractive index at modest fill factors. This metafluid can be synthesized in large-quantity and high-quality and may accelerate development of advanced nanophotonic and metamaterial devices.

15. SUBJECT TERMS

metamaterial, metafluid, nanoparticles, plasmonics, colloidal synthesis, optical-frequency magnetism

16. SECURITY CLASSIFICATION OF:			**17. LIMITATION OF ABSTRACT**	**18. NUMBER OF PAGES**	**19a. NAME OF RESPONSIBLE PERSON**
a. REPORT	**b. ABSTRACT**	**c. THIS PAGE**			Jennifer A. Dionne
UU	UU	UU	UU	10	**19b. TELEPHONE NUMBER** *(include area code)* 650-736-2286

Colloidal Metamaterials at Optical Frequencies

Annual Report, June 30, 2014

A. Investigators

PI: Jennifer Dionne, Assistant Professor of Materials Science and Engineering, Stanford
Funded students and postdocs:
Sassan Sheikholeslami, Postdoctoral Fellow, Materials Science, Stanford University
Hadiseh Alaeian, Graduate Student, Electrical Engineering, Stanford University
Aitzol Garcia-Extarri, Postdoctoral Fellow, Stanford University

B. Abstract

Metamaterials hold enormous potential for controlling the dispersion and propagation of light to achieve properties not found in nature. Fundamentally, these properties arise from the specific arrangement of constituent parts in the material at a scale much shorter than the operating wavelength. To date, almost all reported metamaterials have been fabricated with top- down nanofabrication techniques, which are severely limited in scale and throughput, are inherently limited to planar geometries, and are inherently solid-state materials. Our team has combined theoretical and experimental methods to produce a colloidally-synthesized metamaterial fluid, or "metafluid," exhibiting strong electric and magnetic resonances at visible frequencies. Our metafluid combines the advantages of solution-based processing*(1)* with facile integration into conventional optical components. Protein-antibody interactions are used to direct the solution-phase self-assembly of discrete metamolecules comprised of silver nanoparticles tightly packed around a single dielectric core. The electric and magnetic response of individual metamolecules and the bulk metamaterial solution are directly probed with optical scattering and spectroscopy. Effective medium calculations indicate that the bulk metamaterial exhibits a negative effective permeability and a negative refractive index at modest fill factors. This metafluid can be synthesized in large-quantity and high-quality and may accelerate development of advanced nanophotonic and metamaterial devices.

C. Introduction and Background

More than four decades ago, Victor Veselago considered a hypothetical material in which the electrical permittivity, ε, and the magnetic permeability, μ, were both simultaneously negative.(*2*) His analysis concluded that causality arguments require the index of refraction to be negative, with the remarkable consequence that the phase velocity and energy velocity of light must be in opposite directions. Furthermore, Veselago demonstrated that many familiar optical effects, such as the Doppler shift, Cherenkov radiation, radiation pressure, and Snell's law would all be reversed in such media. At the time, there were no existing materials exhibiting these properties, so interest in this field remained dormant until recent theoretical work published in the last fifteen years. (*3*, *4*)

In a conventional material, the permittivity and permeability arise from the behavior of individual atoms and represent an average response of the material to radiation on a length scale much greater than the atomic spacing. Metamaterials are an extension of this idea, where now an effective permittivity, ε_{eff}, and effective permeability, μ_{eff}, fully

describe the electromagnetic properties of the system on a scale larger than the sub-units. Interest in artificial metamaterials surged in 1999 when John Pendry published results demonstrating that nonmagnetic conductors, structured on scale much smaller than the wavelength of radiation, could exhibit an effective magnetic permeability.(*3*) The split ring resonator (SRR) structures that Pendry originally proposed were based on multiple concentric split rings of conductive material that supported a resonant interaction due to the internal capacitance and inductance of the conductor. The first experimental realization of Pendry's ideas was accomplished by Smith and colleagues in 2000.(*5*)

While fundamentally interesting, SRR-based metamaterials are only readily applicable for wavelengths in the microwave region and longer, due to the difficulty in fabricating such structures at smaller scales, especially three dimensional structures. To date, many groups have explored alternate metamaterial designs with the goal of developing a three dimensional negative index material for visible light. In all successful demonstrations, a negative μ_{eff} was achieved with the combination of conductive and dielectric components structured at a subwavelength scale, using conventional lithographic approaches auch as electron beam lithography (EBL) or focused ion beam (FIB) milling. (*6*, *7*)

Our proposal aimed to design a three-dimensional metamaterial at visible frequencies using bottom-up assembly, to enable highly-scalable and easily-processable metamaterials. Our strategy was to use nanoparticle self-assembly, which has emerged as a powerful technique to generate complex nanostructures with feature sizes on the sub-10-nm scale. (*8-10*) Unlike EBL or FIB, nanoparticle self-assembly has the potential to produce three-dimensional geometries with high throughput and relatively low capital investment. Nanoparticle self- assembly is also compatible with colloidal processing, providing a platform for synthesis of a liquid metamaterial or "metafluid". In contrast to solid-state metamaterials, a metafluid could be directly applied to devices via spincasting or spray-coating for gradient refractive index applications. Alternatively, a metafluid could enable enhanced solution-phase spectroscopy of natural electric, magnetic, or chiral transitions. (*11*, *12*)

D. Results

D.1. Understanding novel coupling between electric and magnetic resonances in colloidal nanostructures

Our funding first enabled thorough investigation of one of the simplest colloidal nanostructure supporting electric and magnetic modes – namely, a trimer of plasmonic nanoparticles. While this structure only supports magnetic modes for one polarization and illumination direction, it's properties provide the platform for designing fully three-dimensional "meta-atoms." Briefly, our work predicted a unique type of electromagnetic coupling between electric and magnetic modes in these discrete nanoparticle clusters**(*13*)**, which has recently been confirmed experimentally**(*14*)**. Our work also demonstrated that both the near and far-field properties of these trimer systems can be strongly tuned based on the symmetry of the structures, for applications ranging from coherent control to active nanophotonic devices and sensors.

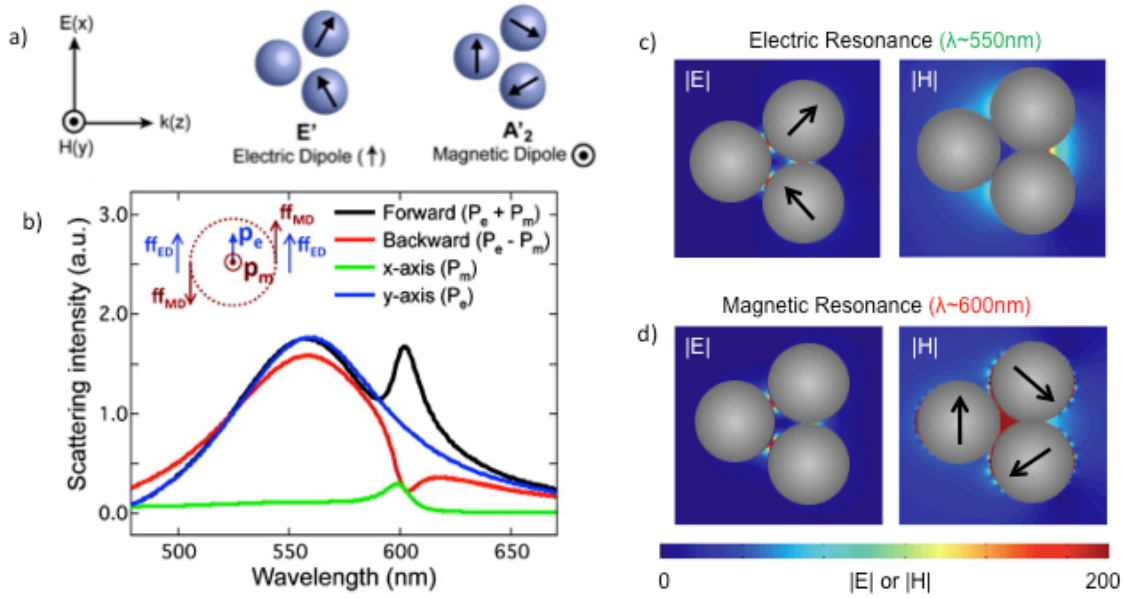

Figure 1. (a) Geometry of excitation. (b) Scattering spectra for different directions for the equilateral trimer. (c) Near-field displacement currents and local electric and magnetic fields for the electric dipolar mode. (d) Near-field displacement currents and local electric and magnetic fields for the magnetic mode.

The near and far-field properties of the plasmonic nanoparticle clusters were calculated using generalized multi-particle Mie (GMM) theory, a fully analytic solution to Maxwell's equations.(*15*) We considered trimers composed of 60 nm diameter silver nanoparticles (optical constants from Johnson and Christy) with a 2 nm interparticle spacing. All calculations were performed assuming an aqueous embedding medium (n = 1.33). For tangential excitation (Figure 1a), both electric and magnetic modes are excited by the incident electric and magnetic fields(16); note that orthogonal excitation only excites electric modes of the trimer.

As seen in Figure 1b, c, and d, this equilateral trimer is characterized by an electric mode for wavelengths near 550nm and a magnetic mode for wavelenths near 600nm. The magnetic mode is characterized by circulating displacement currents and a strongly-enhanced magnetic-field amplitude in the center of the trimer.

The directional scattering spectra of equilateral trimmers is plotted in Figure 1b, and illustrates the strong interference effects between electric and magnetic modes in the forward and backward scattering spectra, which depend on the relative phases of the modes. While the electric fields radiated by the electric dipole are radially symmetric, the electric fields generated by the magnetic dipole are antisymmetric (see inset). In the forward direction, the resulting interference is predominantly constructive, while in the backward direction the interference is almost exclusively destructive. Furthermore, as the individual electric and magnetic dipole moments do not interact in the equilater trimer, scattering in transverse directions (x,y) reveals the unperturbed modes.

Interestingly, geometric variation of trimers enables significant engineering of the near and far-field field of the trimer, based on the interaction between electric and magnetic

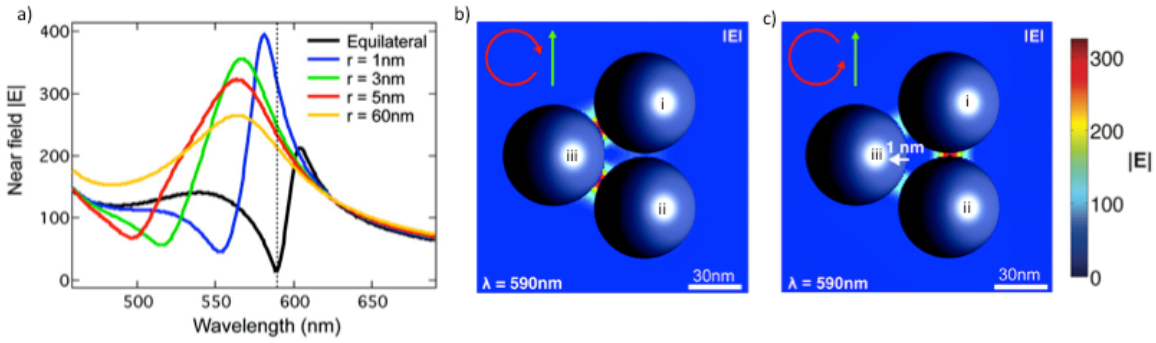

Figure 2 Near-field properties of the tangentially excited trimer as a function of the perturbation parameter, r. (a) The near-field amplitude between particle i and ii as a function of r. The vertical dotted line marks λ = 590 nm. (b) Near-field amplitude map, calculated at all points in the dielectric medium between the particles of the equilateral trimer at λ = 590 nm. (c) Near-field amplitude map for the isosceles trimer with r = 1 nm at λ = 590 nm.

modes. Figure 2 illustrates the near-field properties of trimers with varying degrees of asymmetry. In the figures, particle iii is displaced from the equilateral position by r=0-60nm. The near field amplitude between particles i and ii is plotted in panel a, showing significant spectral tunability and distinct Fano-like lineshapes. These Fano resonances arise from interference between the electric and magnetic modes of the broken symmetry trimer. For larger r, the spectral asymmetry becomes less pronounced as the interaction between modes decreases. Additionally, the phase of the projected electric near field at P2 undergoes a large change as the geometry is shifted (data not shown). The peak in the phase is broadened and shifted and is highly correlated with the dip in the near-field amplitude. The ability to tune both the amplitude and phase of the local fields could be very useful for coherent control applications as well as in the design of nanoscale optoelectronic devices, such as Mach–Zender interferometers, where the local phase of electric and magnetic fields is critical.

As an example of this near-field tunability, Figure 2 plots the near-field of an equilateral trimer and an isosceles trimer with particle iii shifted by 1 nm, at a wavelength of 590nm. Interestingly, due to the strong interference of the electric and magnetic modes, the position and intensity of the 'hotspot' shifts dramatically. From the amplitude information of the near-field response, the field between particles i and ii in the equilateral trimer is strongly suppressed due to the destructive interference, and the strongest field enhancements are located at the junctions between adjacent particles. With just a 1 nm geometrical shift (Figure 2c), however, the field between particles i and ii is significantly enhanced, increasing more than 30-fold as a result of the constructive interference of near fields arising from electric and magnetic modes. Meanwhile, the fields between adjacent particles are strongly suppressed.

The engineering of interactions between electric and magnetic modes in plasmonic systems should have important applications for controlled nanoscale optical emission, as well as in design of novel surface enhanced spectroscopies, ultrasensitive sensors, and active metamaterials.

D.2. Designing a three-dimensional meta-atom with strong electric and magnetic resonances.

Armed with an understanding of the equilateral and isosceles trimer system, we sought to design a colloidal three-dimensional isotropic "meta-molecule" exhibiting electric and magnetic resonances at visible frequencies. Using a suite of stat-of-the-art theoretical methods - including generalized Mie theory, finite difference time domain simulation, and effective medium theory - we sought a meta-atom that would be isotropic (exhibiting electric and magnetic resonances for all angles and polarizations of incident light), and would be synthetically tractable with state-of-the-art colloidal methods.

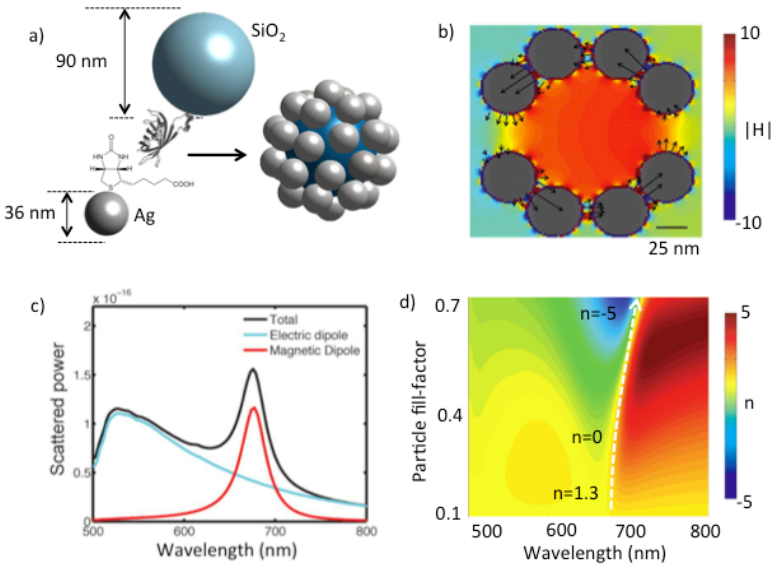

Figure 3. (a) Meta-molecule design. (b)The near-field properties of the metamolecule at the magnetic dipole resonance frequency (668 nm). The cross-sectional colormap shows the near-field magnetic enhancement, while the overlaid arrows display the displacement current between the silver nanoparticles. The strong magnetic field enhancement across the middle of the metamolecule and the circulating displacement currents are a signature of the magnetic dipole mode. (c) Multi-polar decomposition of the scattered fields into the electric and magnetic dipolar contributions. (d) Effective refractive index as a function of wavelength and fill factor.

Figure 3a shows our metamolecule design, consisting of 32 silver nanoparticle spheres (diameter ~ 36 nm) surrounding a 90 nm dielectric core. Our proposed meta-atom is fully isotropic and shows overlapping electric and magnetic modes (figure 3b), crucial for a negative index "metafluid". Our effective medium calculations indicate the effective permittivity, permeability, and refractive index of a bulk medium comprised of these meta-atoms. For reasonable fill-factors, all three parameters can indeed be negative, enabling an isotropic, visible frequency negative-index metafluid.

D.3. Solution-based synthesis and assembly of meta-atoms

We then developed a colloidally-based synthesis of the designed meta-molecules. Standard literature techniques were used to synthesize both silver and polystyrene nanoparticles. Then, the silver nanoparticles were functionalized with a stabilizing layer of polyethylene glycol ligands (to achieve higher stability in biologically relevant buffers) and biotin antibodies. The polystyrene nanoparticles were coated with a layer of streptavidin proteins, which have a very strong affinity to bind to the biotin molecules functionalized on the silver nanoparticles. The meta-molecules were assembled in high yield by mixing the appropriate ratios of the anti-body functionalized silver and protein functionalized polystyrene nanoparticles in a high ionic strength buffer. The assembled

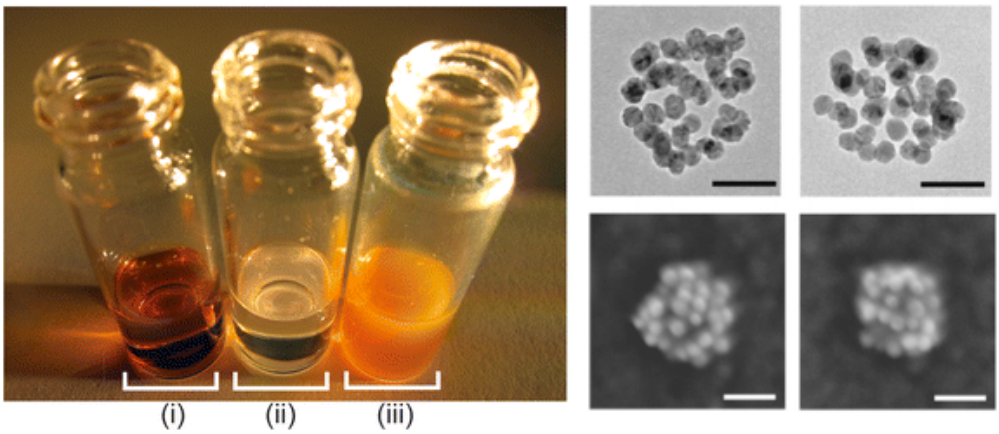

Figure 4 (Left) Photographs of (i) silver nanoparticle solution, (ii) polystyrene nanoparticle solution, (iii) Solution of assembled meta-atoms. (Right) Transmission electron micrographs and scanning electron micrographs of the self-assembled meta-molecules. Scale bars are 100nm.

meta-atoms were then purified from the unreacted starting materials by repeated rounds of centrifugation and filtration. As seen in Figure 4, the metamolecules are made in high-yield with good monodispersity. The three-dimensional structure of the metamolecules is partially evident from the individual scanning electron micrographs. A tomographic tilt series confirms their highly symmetric structures, as visualized in three dimensions at high resolution using transmission electron microscopy.

D.4. Optical characterization of meta-atoms at single particle and ensemble level showing strong optical magnetism

Our team has developed optical techniques to characterize the meta-atoms at the single particle and the ensemble level. These measurements directly confirmed the strong electric and magnetic dipolar modes in the assembled meta-atoms. The single meta-atom measurements were performed in a customized scattering dark-field microscope. A dilute solution of the meta-atoms was introduced into a thin liquid cell atop an inverted microscope, allowing the particles to remain in the fluid-phase (see figure 5, top). With p-polarized excitation, the light scattered from individual meta-atoms was collected and analyzed in a spectrometer. When collecting light of all polarizations, the scattering contains contributions from all allowed modes with a shoulder on the low energy side centered at 700 nm, indicative of the magnetic mode. To confirm the magnetic nature of this peak in the unpolarized spectrum, we used an additional polarizer on the detection side. This setup eliminates most of the contribution from the electric dipolar mode, revealing the magnetic mode near 700 nm. The experimental dark-field measurements are in excellent agreement with the theoretical calculations.

The optical magnetism of the bulk liquid metamaterial was probed using a home-built angle and polarization resolved light scattering setup, shown in figure 6. A polarized laser is sent down a test tube filled with a solution of the metamolecules, and the polarization-filtered light is collected by a photodetector as a function of angle in 5° increments. The light scattered by magnetic dipoles will have a cosine-squared dependence, polarized axially with respect to the incident beam. In contrast, the light scattered by electric

dipoles will have a sine-squared dependence that is transversely polarized with respect to the incident beam. This measurement can therefore directly quantify the magnetic dipole of the colloidal metamaterial.

Since the metamolecules are suspended in water (n = 1.33), the magnetic resonance is predicted to blue shift from 668 nm (as calculated in Figure 3c) to 631 nm. Accordingly, we probe the magnetic dipole of the ensemble metafluid using a polarized HeNe source at 633 nm. Note that scattering from electric quadrupoles is minimal at this wavelength.

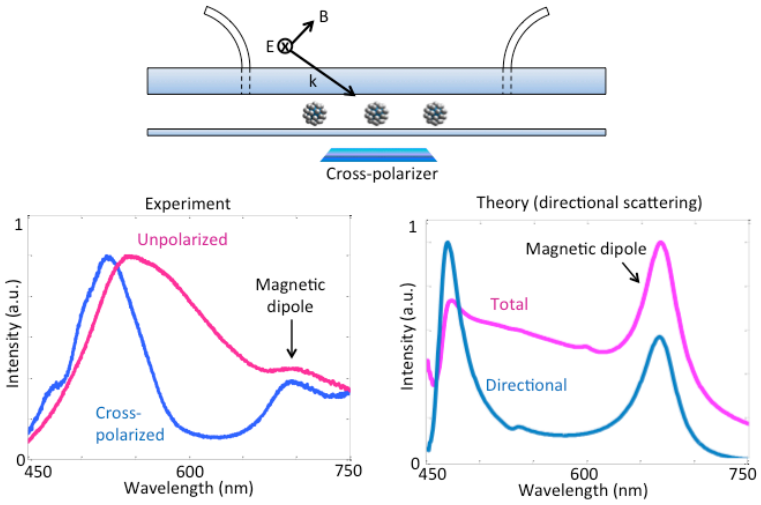

Figure 5. (Top) Experimental dark-field setup to measure scattering from an individual metamolecule, considering both unpolarized and cross-polarized configurations. The cross-polarized configuration filters out the scattering from the electric dipolar mode, revealing the magnetic dipolar contribution. (Bottom) Dark-field scattering spectra for a single meta-atom with unpolarized and cross-polarized detection. The theoretically calculated scattering spectra shows excellent agreement with the experiment.

The right panel of Figure 6 plots the normalized scattering intensity from the self-assembled colloidal metamaterial and from a control sample consisting of the same number and concentration of unassembled silver and dielectric particles. Note that the very small magnetic dipole scattering from the control (unassembled) sample originates from the first order magnetic Mie type mode of the dielectric particle. The substantial magnetic dipole scattering from the assembled metamaterial is approximately 12% of the strength of the electric dipole scattering and more than an order of magnitude greater than the control sample. To our knowledge, this measurement is the first direct evidence of magnetic dipole scattering in a bulk colloidal metamaterial liquid. Ongoing work is aimed at directly measuring the effective permittivity, permeability, and refractive index of the fluid, and creating a negative index fluid.

G. Conclusions

Using a suite of analytic calculations, electrodynamic simulations, and state-of-the-art experimental techniques, our project has: 1) predicted a new type of mode coupling between electric and magnetic modes; 2) designed an isotropic meta-atom using metallic and dielectric nanospheres, exhibiting the potential for bulk negative refractive indices; 3) synthesized these meta-atoms in solution at the gram-scale; and 4) developed optical measurements to directly quantify the coexistence of electric and magnetic modes in this system at both the single meta-atom and bulk fluid level.

Importantly, our colloidal approach to metamaterial synthesis produces three-dimensional structures with nanoscale precision, free from the constraints of conventional, top-down

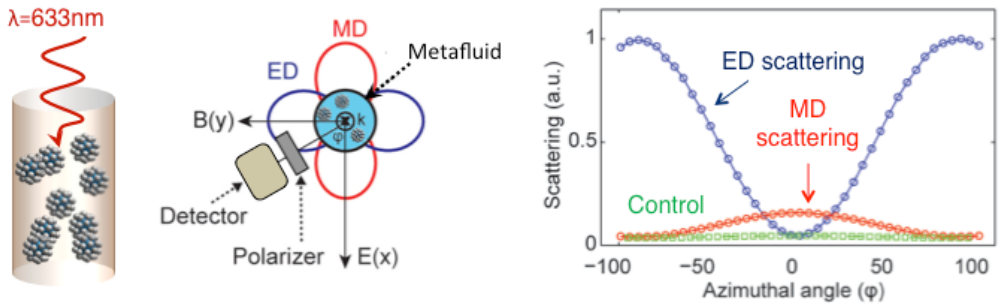

Figure 3. Optical characterization of the bulk metafluid. The left panels show the experimental setup. The electric and magnetic modes are distinguished by angle and polarization-resolved scattering. The right-most panel shows the experimental data collected for the assembled metafluid and the control sample (unassembled silver and polystyrene, with identical concentrations). The strong scattering of the magnetic dipole mode in the assembled metafluid is 12% of the strength of the electric mode.

lithographic methods. Our liquid metamaterial could form the basis for new tunable or gradient-index media, applied either as a gel-coating onto solid-state devices or integrated into microfluidic cells. The metamaterial could also create new opportunities for enhanced solution-phase spectroscopy of electric, magnetic, or chiral transitions. Further, based on their facile large-scale synthesis, these fluid materials might accelerate the evolution of metamaterials from an academic pursuit to an industrial technology.

G. Publications resulting from funding

S. Sheikholeslami, H. Alaeian, A. L. Koh, J. A. Dionne, "A metafluid exhibiting strong optical magnetism." *Nano Letters*, 2013. (13) 4137-4141.

S. Sheikholeslami, A. Garcia-Etxarri, J. A. Dionne, "Controlling the interplay of electric and magnetic modes via Fano-like plasmon resonances." *Nano Letters*, 2011. (11) 3927-3934.

H. Alaeian and J. Dionne, "Plasmon nanoparticle superlattices as optical-frequency magnetic metamaterials," Optics Express, Vol. 20 (14), pp. 15781-15796, 2012

A. Atre, A. Garcia, H. Alaeian and J. Dionne, "A broadband negative index metamaterial at optical frequencies," Advanced Optical Materials, Vol. 1 (4), pp. 327-333, 2013.

J. Scholl, A. Garcia-Etxarri, A. Koh and J. Dionne, "Observation of quantum tunneling between two plasmonic nanoparticles," *Nano Letters* Vol. 13 (2), pp. 564-569, 2013.

F. References

1. J. A. Fan *et al.*, Self-Assembled Plasmonic Nanoparticle Clusters, *Science* **328**, 1135–1138 (2010).

2. V. G. Veselago, Electrodynamics of media with simultaneously negative magnetic and electric permeabilities, *Sov Phys—Usp* (1968).

3. J. Pendry, A. Holden, D. Robbins, W. Stewart, Magnetism from conductors and enhanced nonlinear phenomena, *Ieee T Microw Theory* **47**, 2075–2084 (1999).

4. J. Pendry, Negative refraction makes a perfect lens, *Phys Rev Lett* **85**, 3966–3969 (2000).

5. D. Smith, W. Padilla, D. Vier, S. Nemat-Nasser, S. Schultz, Composite Medium with Simultaneously Negative Permeability and Permittivity, *Phys Rev Lett* **84**, 4184–4187 (2000).

6. H. J. Lezec, J. A. Dionne, H. A. Atwater, Negative Refraction at Visible Frequencies, *Science* **316**, 430–432 (2007).

7. S. Linden *et al.*, Photonic metamaterials: Magnetism at optical frequencies, *Ieee J Sel Top Quant* **12**, 1097–1105 (2006).

8. C. M. Soukoulis, M. Wegener, Past achievements and future challenges in the development of three-dimensional photonic metamaterials, *Nat Photonics* **5**, 523–530 (2011).

9. A. V. Pinheiro, D. Han, W. M. Shih, H. Yan, Challenges and opportunities for structural DNA nanotechnology, *Nat Nanotechnol* **6**, 763–772 (2011).

10. S. J. Barrow, X. Wei, J. S. Baldauf, A. M. Funston, P. Mulvaney, The surface plasmon modes of self-assembled gold nanocrystals, *Nat Commun* **3**, 1275 (2012).

11. S. Karaveli, R. Zia, Spectral Tuning by Selective Enhancement of Electric and Magnetic Dipole Emission, *Phys Rev Lett* **106**, 193004 (2011).

12. N. Noginova, G. Zhu, M. Mavy, M. A. Noginov, Magnetic dipole based systems for probing optical magnetism, *J Appl Phys* **103**, 07E901 (2008).

13. S. N. Sheikholeslami, A. Garcia-Etxarri, J. A. Dionne, Controlling the Interplay of Electric and Magnetic Modes via Fano-like Plasmon Resonances, *Nano Lett* **11**, 3927–3934 (2011).

14. F. Shafiei *et al.*, A subwavelength plasmonic metamolecule exhibiting magnetic-based optical Fano resonance, *Nat Nanotechnol* **8**, 95–99 (2013).

15. Y. XU, ELECTROMAGNETIC SCATTERING BY AN AGGREGATE OF SPHERES, *Appl Optics* **34**, 4573–4588 (1995).

16. Y. A. Urzhumov *et al.*, Plasmonic nanoclusters: a path towards negative-index metafluids, *Opt Express* **15**, 14129–14145 (2007).